

# RSC Advances



This is an *Accepted Manuscript*, which has been through the Royal Society of Chemistry peer review process and has been accepted for publication.

*Accepted Manuscripts* are published online shortly after acceptance, before technical editing, formatting and proof reading. Using this free service, authors can make their results available to the community, in citable form, before we publish the edited article. This *Accepted Manuscript* will be replaced by the edited, formatted and paginated article as soon as this is available.

You can find more information about *Accepted Manuscripts* in the [Information for Authors](#).

Please note that technical editing may introduce minor changes to the text and/or graphics, which may alter content. The journal's standard [Terms & Conditions](#) and the [Ethical guidelines](#) still apply. In no event shall the Royal Society of Chemistry be held responsible for any errors or omissions in this *Accepted Manuscript* or any consequences arising from the use of any information it contains.

**Determination of losartan potassium in the presence of hydrochlorothiazide *via* combination of magnetic solid phase extraction, and fluorimetry techniques in urine sample**

Amir Farnoudian-Habibi<sup>1</sup>, Sahar Kangari<sup>2</sup>, Bakhshali Massoumi<sup>3</sup>, and Mehdi Jaymand<sup>\*, 1</sup>

1. Research Center for Pharmaceutical Nanotechnology, Tabriz University of Medical Sciences, P.O. Box: 51656-65811, Tabriz, Islamic Republic of Iran.
2. Department of Chemistry, Science and Research Branch, Islamic Azad University, P.O. Box: 14515-775, Tehran, Islamic Republic of Iran.
3. Department of Chemistry, Payame Noor University, P.O. BOX: 19395-3697, Tehran, Islamic Republic of Iran.

---

\* Correspondence to: Mehdi Jaymand, Research Center for Pharmaceutical Nanotechnology, Tabriz University of Medical Sciences, Tabriz, Islamic Republic of Iran.

Tel: +98-41-33367914; Fax: +98-41-33367929

Postal address: Tabriz-5165665811-Iran

E-mail addresses: [m\\_jaymand@yahoo.com](mailto:m_jaymand@yahoo.com); [m.jaymand@gmail.com](mailto:m.jaymand@gmail.com); [jaymandm@tbzmed.ac.ir](mailto:jaymandm@tbzmed.ac.ir)

**Abstract**

A sensitive and highly efficient method for determination of losartan potassium (LOS) in the presence of hydrochlorothiazide (HCTZ) *via* combination of magnetic solid phase extraction (MSPE), and fluorimetry techniques is suggested. For this purpose, the imidazolium ionic liquid (Imz)-modified  $\text{Fe}_3\text{O}_4@\text{SiO}_2$  nanoparticles ( $\text{Fe}_3\text{O}_4@\text{SiO}_2\text{-Imz}$ ) was utilized as an adsorbent for the MSPE. The  $\text{Fe}_3\text{O}_4@\text{SiO}_2\text{-Imz}$  exhibited excellent extraction performance for LOS, in part due to its anion-exchange groups in Imz moiety. The experimental parameters such as sample pH values, the amount of adsorbent, extraction time, desorption solvent, and desorption time that could affect the extraction performance, were examined and optimized. Determination of LOS in the presence of HCTZ in urine sample was carried out by selective and sensitive excitation-emission fluorescence spectroscopy (EEFS), because only LOS exhibited fluorescence emission in 325 nm, while the HCTZ did not exhibit any fluorescence emission. The limit of detection (LOD) for LOS by this technique was obtained  $0.12 \text{ ngml}^{-1}$ .

**Keywords:** Losartan; Hyrdochlorothiazide; Magnetic solid phase extraction; Fluorimetry; Urine sample

## 1. Introduction

Losartan potassium salt (2-n-butyl-4-chloro-5-hydroxymethyl-1-[(2%-(1H-tetrazol-5-yl) biphenyl-4-yl)methyl]imidazole) is a prototype of a new generation of effective and orally active non-peptide angiotensin II receptor antagonists. These substances have been developed in sequence to the angiotensin converting enzyme inhibitors as a further therapeutic action on the renin-angiotensin-aldosterone system, one of the most important regulators of blood pressure.<sup>1,2</sup> It is well established that the 5-carboxylic acid metabolite of losartan is a potent angiotensin II antagonist.<sup>3-5</sup> Hydrochlorothiazide (HCTZ), or 6-chloro-3,4-dihydro-2H-1,2,4-benzothiadiazine-7-sulfonamide 1,1-dioxide, is a diuretic of the class of benzothiadiazines widely used in antihypertensive pharmaceutical formulations, alone or in combination with other drugs, which decrease active sodium re-absorption, and reduce peripheral vascular resistance. These two mentioned drugs (LOS and HCTZ) are commonly used in association in the treatment of hypertension.<sup>6,7</sup> The chemical structures of these drugs are shown in Scheme 1.

Several analytical methods such as high-performance liquid chromatography (HPLC),<sup>8,9</sup> reversed phase HPLC (RP-HPLC),<sup>10,11</sup> LC-MS,<sup>12,13</sup> colorimetry,<sup>14</sup> complex formation,<sup>15,16</sup> charge-transfer complexes,<sup>17</sup> and capillary electrophoresis (CE)<sup>18</sup> have been applied for the determination of LOS in the presence of HCTZ. On the other hand, in last decade a great deal of research efforts have been focused on the development of new, and efficient methods for extraction, concentration, and isolation of real samples to enhance sensitivity, and selectivity of the analytical methods. In this regard, the solid phase extraction (SPE) can be considered as an efficient and versatile

approach, in part due to its improvements in automation, reproducibility, and high-throughput capability.<sup>19-21</sup>

However, the request for new adsorbents is an important factor in improving analytical sensitivity, and precision in SPE technique. To date, many adsorbents, such as active carbon,<sup>22</sup> modified resin,<sup>23</sup> fullerene,<sup>24</sup> and conductive polymers<sup>25,26</sup> have been employed in SPE. A relatively novel achievement in the field of SPE is the use of magnetic nanoparticles (MNPs), which is the so-called magnetic solid phase extraction (MSPE). The some advantages of MSPE method over SPE can be listed as: excellent adsorption efficiency, rapid separation from the matrix through external magnetic field without retaining residual magnetization after its removal, and has recently exhibited significant advantages in separation science.<sup>27-29</sup>

This paper describes a novel, sensitive, and selective method for the determination of losartan potassium (LOS) in the presence of hydrochlorothiazide (HCTZ) in human urine sample. According to the drug loading process (as described in Experimental section), it was found that HCTZ had an interfering role in this study, due to its low loading on the adsorbent surface, and no exhibition of fluorescence emission. Hence, we optimized all parameters such as pH values, the amount of adsorbent, extraction time, desorption solvent, and desorption time for MSPE, and determination of LOS.

### (Scheme 1)

## 2. Experimental

### 2.1. Material

All chemicals including, methanol, acetonitrile,  $\text{FeCl}_3 \cdot 6\text{H}_2\text{O}$  (99%),  $\text{FeCl}_2 \cdot 4\text{H}_2\text{O}$  (98%), tetraethylorthosilicate (TEOS) (98%), and 3-chloropropyltrimethoxysilane (CPTMS) were of analytical reagent grade or the highest purity available from Merck

(Darmstadt, Germany). Double distilled water (DDW) was utilized throughout the study. Standard solutions of LOS and HCTZ were prepared daily with dissolving of 0.1 mg of them in 100 ml DDW. The 0.1 mol<sup>-1</sup> solution of NaOH for pH adjustment obtained through dilution of Merck standard solution of it. All of the solutions were prepared daily, and drug solutions were kept in 5 °C.

## 2.2. Synthesis of Fe<sub>3</sub>O<sub>4</sub>@SiO<sub>2</sub> core-shell nanoparticles

Magnetite NPs were prepared by chemical co-precipitation method under alkaline condition.<sup>30</sup> In order, the molar ratio of Fe<sup>2+</sup> to Fe<sup>3+</sup> salts was maintained at 1:2. In a typical synthesis, FeCl<sub>3</sub>.6H<sub>2</sub>O (5.4 g, 20 mmol) and FeCl<sub>2</sub>.4H<sub>2</sub>O (1.95 g, 10 mmol) were dissolved in DDW (50 ml) with vigorous stirring. The solution was deoxygenated by bubbling highly pure argon gas for 20 minutes, and then was heated to 80 °C. After vigorous stirring for about 1 hour, 20 ml of NH<sub>4</sub>OH (28 wt.%) was added dropwise. The resultant suspension was maintained at 80 °C for another 1 hour with vigorous stirring, and then cooled to room temperature. The black powder was collected by an external magnetic field, washed with 50% aqueous ethanol for several times, and dried under vacuum at 80 °C.

In order to obtain the well-dispersed Fe<sub>3</sub>O<sub>4</sub> NPs, the prepared MNPs were added on citric acid (10 ml, 0.1 mol<sup>-1</sup>) and sonicated for 30 minutes. The reaction was maintained for 12 hours at room temperature with vigorous stirring, and at the end of this time, the product was washed several times by DDW. The obtained citrate-coated MNPs (CMNPs) were separated with external magnetic field. It is important to note that the citric acid was used as a coating agent for colloidal stabilization of MNPs in aqueous solution.

The Fe<sub>3</sub>O<sub>4</sub>@SiO<sub>2</sub> core-shell NPs were prepared by the growth of a silica layer on Fe<sub>3</sub>O<sub>4</sub> NPs. Therefore, the obtained CMNPs (1.0 g) were added on 10% aqueous ethanol solution (20 ml), and the mixture sonicated for 20 minutes. Under continuous stirring, ammonia solution (28 wt.%; 5 ml), and tetraethoxyorthosilicate (TEOS, 5 ml) were added to the reaction mixture. The resulting mixture was stirred under N<sub>2</sub> atmosphere for 12 hours at room temperature. Then, the core-shell NPs were separated by an external magnetic field to eliminate the homogeneous silica nucleus. The product washed several times with water, and ethanol, and dried overnight under vacuum at room temperature.

### 2.3. Synthesis of Fe<sub>3</sub>O<sub>4</sub>@SiO<sub>2</sub>-Imz

The obtained Fe<sub>3</sub>O<sub>4</sub>@SiO<sub>2</sub> core-shell NPs (1 g) were dispersed in methanol (50 ml) and toluene (5 ml) mixture under sonication for about 20 minutes, and then, 3-chloropropyltrimethoxysilane (CPTMS, 2 ml) was added dropwise to the reaction mixture. The reaction mixture was stirred for about 48 hours under argon atmosphere, and then centrifuged, washed several times with methanol, and dried overnight under vacuum at room temperature. Afterward, the CPTMS-modified Fe<sub>3</sub>O<sub>4</sub>@SiO<sub>2</sub> nanoparticles (0.6 g) were added on solution of imidazole (0.7 g, 10 mmol) in CHCl<sub>3</sub> (50 ml), and the suspension was refluxed for 24 hours at 50°C. The obtained brownish nanoparticles were washed by CHCl<sub>3</sub> (3×20 ml), and dried under vacuum at room temperature.<sup>31</sup>

### 2.4. Solid phase extraction and preconcentration

Briefly, Fe<sub>3</sub>O<sub>4</sub>@SiO<sub>2</sub>-Imz nanoparticles (1 mg) were activated with 10 ml of NaOH solution (0.01 mol l<sup>-1</sup>) for about 12 hours, and then washed with DDW for several times. Then, 250 ml (0.1 mg l<sup>-1</sup>) of LOS-HCTZ mixture (pH was adjusted at 8 by 0.1

mol<sup>-1</sup> of NaOH solution) was added. After vigorous stirring for about 10 minutes, adsorbent was collected using external magnetic field. Spectrophotometric results indicated the loading efficiency of 99% and 44% for LOS and HCTZ, respectively. The adsorption percent (%R<sub>e</sub>) was determined using the following equation:

$$\%R_e = \frac{[C_0 - C_e]}{C_0} \times 100$$

where C<sub>0</sub> and C<sub>e</sub> represent the initial and final (after adsorption) concentration of species, respectively. After discarding the supernatant, 2 ml of desorption solution (a mixture of methanol and NaOH (20% w/v)) was added to the system, and stirred for about 15 minutes to desorption of loaded drugs. After desorption process, the solution was decanted, and injected into fluorometer equipment for more analysis.

## 2.5. Instrumentation

The magnetic properties of the samples were investigated using vibrating-sample magnetometer (VSM, AGFM, Iran) at room temperature. Scanning electron microscopy (SEM) images were collected by a LE 440I SEM (Oxford, UK) scanning electron microscope. The samples for SEM imaging were coated with a thin layer of gold film to avoid charging. X-ray diffraction (XRD) spectra were obtained with a Siemens D 5000 (Aubrey, Texas, USA), X-ray generator (CuK<sub>α</sub> radiation with λ=1.5406Å) with a 2θ scan range of 2 to 80° at room temperature. Fluorescence spectra were recorded using a FP-6200 spectrofluorometer (JASCO Corporation, Tokyo, Japan) with a wavelength range of 100–400 nm (with 1 nm intervals) for excitation. The instrument was equipped with a 150 W xenon lamp and dual monochromators (silicon photodiode for excitation and photomultiplier for emission).

The slit widths for both excitation and emission were set at 5 nm, and the fluorescence spectra were recorded at a scan rate of 250 nm min<sup>-1</sup>.

### 3. Results and discussion

#### 3.1. Characterization of Fe<sub>3</sub>O<sub>4</sub>@SiO<sub>2</sub>-Imz

The X-ray diffraction pattern of the Fe<sub>3</sub>O<sub>4</sub>@SiO<sub>2</sub>-Imz nanoparticles is shown in Figure 1. All of the observed diffraction peaks are indexed by the cubic structure of the Fe<sub>3</sub>O<sub>4</sub> nanoparticles. As can be seen, the XRD pattern of the Fe<sub>3</sub>O<sub>4</sub>@SiO<sub>2</sub>-Imz nanoparticles are in agreement with the standard Fe<sub>3</sub>O<sub>4</sub> structure, and indicated that these particles have phase stability, and also the structural integrity was preserved. The diffraction peaks at 2θ=29.7, 35.5, 43.2, 53.2, 57.1, 62.2, and 74.3° are correspond to the (220), (311), (400), (422), (511), (440), and (533) of Fe<sub>3</sub>O<sub>4</sub> crystalline structure, respectively. In addition, a broad diffraction peak in range of 2θ=5 to 20° is may be attributed to the amorphous silica layer.

To have a better visual insight into the morphology of the synthesized Fe<sub>3</sub>O<sub>4</sub>@SiO<sub>2</sub>-Imz nanoparticles scanning electron microscopy (SEM) image is observed. Figure 2 shows the SEM image of the Fe<sub>3</sub>O<sub>4</sub>@SiO<sub>2</sub>-Imz nanoparticles. As seen in this image the average diameter of the nanoparticles is ~20 nm.

The magnetic properties of the Fe<sub>3</sub>O<sub>4</sub>@SiO<sub>2</sub>-Imz nanoparticles were characterized by means of vibrating sample magnetometer (VSM). The typical room temperature magnetization curve bare of the Fe<sub>3</sub>O<sub>4</sub>@SiO<sub>2</sub>-Imz is shown in Figure 3. According to this figure, the magnetic saturation value of the Fe<sub>3</sub>O<sub>4</sub>@SiO<sub>2</sub>-Imz nanoparticles is 46 emu g<sup>-1</sup>.

(Figure 1)

(Figure 2)

(Figure 3)

### 3.2. Optimization of MSPE process

In order to achieve the high extraction and preconcentration efficiency, the factors affecting the adsorption, and desorption processes such as the amount of adsorbent, eluent type, desorption time, pH value, and sample volume were optimized. The results obtained were discussed in following sections.

#### 3.2.1. Effect of pH

Sample pH is a critical factor regarding extraction efficiency, since, it determines the ionic or neutral state of the molecules and also change or improve the charge of species which influence the interaction force with adsorbent. The effect of sample pH on the performance of MSPE was investigated in the range of 3.0 to 10.0 for 1 mg of adsorbent, and 10 ml standard solution of drugs mixture ( $0.1 \text{ mg l}^{-1}$  for each drug). As shown in Figure 4, when the other conditions were constant, the pH values strongly affected the extraction of LOS. The extraction performance improved with the increasing of pH values, and reached the maximum (99%) at pH value 8.0, then decreased when the pH values increased continuously. This interesting changed trend can be explained as follows: according to the chemical structure of LOS, it is potassium salt and in all investigated pHs has negative charge, hence it could be loaded on adsorbent. But in  $\text{pH} > \text{pK}_a$  of LOS (5.5) loading is increased. With the increasing of pH values, chlorine ions ( $\text{Cl}^-$ ) in the  $\text{Fe}_3\text{O}_4@\text{SiO}_2\text{-Imz}$  were replaced by hydroxyl ( $\text{OH}^-$ ) groups, which meant more and more imidazolium groups were activated. Therefore, the anion-exchange interaction between  $\text{Fe}_3\text{O}_4@\text{SiO}_2\text{-Imz}$ , and LOS was stronger, and led to the improvement of the extractive performance.

However, excess OH groups would compete with the ion-exchange sites on the  $\text{Fe}_3\text{O}_4@\text{SiO}_2\text{-Imz}$  when the pH values increased continuously. Therefore, higher pH value did not favor for the extraction of anions. According to the results, setting the pH values of matrix at 8.0 was used in present research. Nevertheless, the results indicated that the HCTZ has almost constant manner (maximum loading approximately 44%) in all of pH values. It was due to, HCTZ ( $\text{pK}_a=9.98$ ) is a neutral species in investigated pH range, and HCTZ–adsorbent interactions must be mostly of the polar or  $\pi$ – $\pi$  type rather than ionic type. According to the mentioned detail we concluded that LOS had a stronger ionic interaction with adsorbent, and saturated its surface better and stronger than HCTZ. Thus, HCTZ had an interference role in this study, due to its low loading on adsorbent surface, and as mentioned previously no exhibition of fluorescence emission.

(Figure 4)

### 3.2.2. Effect of $\text{Fe}_3\text{O}_4@\text{SiO}_2\text{-Imz}$ amount and contact time

Preconcentration of targeted drug (LOS) is generally influenced by the amount of the  $\text{Fe}_3\text{O}_4@\text{SiO}_2\text{-Imz}$  adsorbent material. The effect of the adsorbent amount on the extraction efficiency was studied in the range of 0.25 to 1.5 mg. As shown in Figure 5, with the amount increasing of  $\text{Fe}_3\text{O}_4@\text{SiO}_2\text{-Imz}$ , the extraction efficiency enhanced to 99% by adding 10 ml ( $0.1 \text{ mg l}^{-1}$ ) of drugs mixture on investigated weights of adsorbent. In addition, according to Figure 6, the optimum contact time was obtained 10 minutes.

(Figure 5)

(Figure 6)

### 3.3. Equilibrium adsorption study

The adsorption isotherm is defined as the relationship between the amount of a substance adsorbed per unit mass of an adsorbent at given temperature, and its concentration in the equilibrium solution. It is well established that the adsorption isotherm is an essential way to describe how solutes interact with the sorbent. Developing an appropriate isotherm model for adsorption is essential to the design and optimization of adsorption processes. In this respect several isotherm models such as Langmuir, Freundlich, Redlich–Peterson, Dubinin–Radushkevich, Sips, and Temkin have been developed for evaluating the equilibrium adsorption of compounds from solutions.<sup>32</sup> However, the most commonly used model to investigation of the adsorption isotherm is Langmuir equation. Thus, the experimental results of this study were fitted with this model. The equilibrium adsorption isotherm is important in determining the adsorption capacity of LOS and diagnoses the nature of adsorption onto the Fe<sub>3</sub>O<sub>4</sub>@SiO<sub>2</sub>-Imz nanoparticles. The equilibrium adsorption capacity of the adsorbent was calculated by the following equation:

$$q_e = \frac{V(C_0 - C_e)}{W}$$

where  $q_e$  is the equilibrium adsorption capacity ( $\text{mgg}^{-1}$ ),  $C_0$  is the initial concentration of the LOS ( $\text{mgL}^{-1}$ ),  $C_e$  is the equilibrium concentration of LOS ( $\text{mgL}^{-1}$ ),  $V$  is the volume of LOS solution (l), and  $W$  is the weight of the adsorbent (g). The equilibrium adsorption of LOS solutions by adsorbent was measured ( $C_0$  of LOS = 0, 5, 10, 15, 20, 50, 100, 200, and 300  $\text{mgL}^{-1}$ ) after equilibrium time. The well known Langmuir equation, which is valid for monolayer sorption on a surface with a finite number of identical sites, is given by the following equation:

$$\frac{C_e}{q_e} = \frac{C_e}{q_{max}} + \frac{K_{ads}}{q_{max}}$$

where  $q_{max}$  is the maximum adsorption at monolayer ( $\text{mgg}^{-1}$ ), and  $K_{ads}$  is the Langmuir constant related to the affinity of binding sites ( $\text{mg}^{-1}$ ) (Figure 7).<sup>33</sup> A linearized plot of  $C_e/q_e$  against  $C_e$  gives  $q_{max}$  and  $K_{ads}$ . The essential characteristics of the Langmuir isotherm can also be expressed in terms of a dimensionless constant of separation factor or equilibrium parameter ( $R_L$ ) which is defined as follows:

$$R_L = \frac{1}{1+bC_0}$$

where  $b$  is the Langmuir constant. The  $R_L$  value indicates the shape of isotherm.<sup>34</sup> The  $R_L$  values between 0 and 1 indicate favorable adsorption, while  $R_L \geq 1$ , and  $R_L = 0$  indicate unfavorable, linear, and irreversible adsorption isotherms. The results obtained from equilibrium adsorption study are summarized in Table 1.

(Figure 7)

(Table 1)

### 3.4. Desorption and preconcentration

The various parameters such as type and volume of the solvent, volume of the sample, and desorption time that could affect the drugs desorption efficiency from the  $\text{Fe}_3\text{O}_4@\text{SiO}_2\text{-Imz}$  nanoparticles were studied, and optimized in the following sections.

#### 3.4.1. Type of desorption solvent

In order to obtain high desorption efficiency of LOS from  $\text{Fe}_3\text{O}_4@\text{SiO}_2\text{-Imz}$  nanoparticles, different organic solvents such as methanol, acetonitrile, ethanol, dioxane, and *n*-hexane were tested, and results obtained was summarized in Table 2.

As seen in this table a mixture of methanol/NaOH (20% w/v) was found as the best eluent for desorption of LOS from Fe<sub>3</sub>O<sub>4</sub>@SiO<sub>2</sub>-Imz nanoparticles.

**(Table 2)**

#### **3.4.2. Desorption solvent volume, and desorption time**

The effect of desorption solvent volume (methanol/NaOH (20% w/v)) on the recovery of the LOS was investigated in the range of 0.5 to 2 ml. As seen in Figure 8, the recoveries have significant increase from 0.5 to 1.0 ml, but had no significant differences between 1.0 to 2.0 ml. So, 1 ml mixture of methanol/NaOH (20% w/v) was selected as an optimum volume for desorption process. In addition, as seen in Figure 9, as optimum time 15 minutes seems to be enough to obtain the maximum efficiency (98%) for the desorption of LOS from Fe<sub>3</sub>O<sub>4</sub>@SiO<sub>2</sub>-Imz nanoparticles.

**(Figure 8)**

**(Figure 9)**

#### **3.4.3. Sample volume effect**

In order to estimate the preconcentration efficiency, sample volume was ranged in 10-350 ml (V= 10, 50, 100, 150, 200, 220, 250, 260, 300, 350 ml). For this purpose, 10 ml mixture solution of drugs (0.1 mg l<sup>-1</sup>) was added on 1 mg of adsorbent, and final sample volume adjusted in range of 10 to 350 ml by adding of DDW. After 10 minutes stirring, spectrophotometric results indicated that in 250 ml of sample volume, LOS loading was > 95 %, but in higher volumes, efficiency of loading was lesser than 93% (Figure 10). Hence, 250 ml was selected as an optimum sample volume. Therefore, for determination of LOS quantities in samples, a sample volume of 250 ml was selected in order to increase the preconcentration factor.<sup>35,36</sup>

**(Figure 10)**

### 3.5. Determination of losartan

As known the LOS has fluorescence emission at 325 nm (excited at 250 nm), whereas we find that the HCTZ did not exhibit any fluorescence emission. This matter is the base of selective determination of LOS in the presence of HCTZ. It should be pointed out that, we were recorded the excitation-emission fluorescence spectra of the mixture of LOS/HCTZ solution, and only emission of LOS without any decrease in intensity or shift in emission maximum was observed. Figure 11, is shown the excitation-emission fluorescence ( $\lambda_{\text{exc}}=250$  nm,  $\lambda_{\text{emi}}=325$  nm) spectra of the LOS.

(Figure 11)

#### 3.5.1. Interference studies

The influences of common interfering species in urine sample such as uric acid, oxalate, phosphate, L-leucine, and glucose were investigated prior to the application of this method in real sample, and the results obtained are summarized in Table 3. It is important to note that, the loading capacity of adsorbent is very high, in part due to its nanostructured morphology and large surface-area. Thus, these interferences did not decrease the loading efficiency of the LOS or HCTZ. On the other hand, as mentioned previously the LOS had very high loading efficiency (99%), in part due to its strong ionic interaction with adsorbent. Furthermore, during extraction and dilution process the interferences concentrations are significantly decreased. For example, in desorption step uric acid and particularly oxalate had low desorption efficiency (45, and 30%, respectively) in comparison with LOS (98%). This may be originated from strong interaction of uric acid and oxalate with adsorbent surface or low tendency to eluent. According to the yielded information from this step, low quenching effect of oxalate and uric acid on LOS fluorescence intensity is expected. It should be pointed

out that, according to Table 3 the tolerance limit was defined as the concentrations which give an error of  $\leq 5\%$  in the determination of LOS. Thus these species do not significantly interfere with the proposed method.

(Table 3)

### 3.5.2. Urine sample preparation

To 1.0 ml of urine sample, the internal standard, LOS and HCTZ ( $0.8 \text{ mg l}^{-1}$ ), and 0.5 ml of  $0.6 \text{ mol l}^{-1}$  sodium carbonate-sodium bicarbonate buffer (pH 9.8) were added. After addition of ethyl acetate/*n*-heptane (5 ml; 80/20 v/v), the vials were capped and mixed vigorously for 2 minutes, then centrifuged at 5000 rpm for 10 minutes. The organic layer was transferred to another tube containing 0.50 ml of acidic phosphate buffer ( $0.025 \text{ mol l}^{-1}$  potassium dihydrogen phosphate adjusted to pH 2.4 with 85% phosphoric acid), then mixed for 1 minute, and centrifuged at 5000 rpm for 10 minutes. The organic layer was discarded, and a 20  $\mu\text{l}$  aliquot of the aqueous phase was injected for preconcentration (final concentration is  $0.1 \text{ mg l}^{-1}$ ). Then 10 ml of resultant was diluted to 250 ml by DDW and used for preconcentration and determination steps.

### 3.5.3. Analytical assay

Under the optimized conditions the limit of detection (LOD) for LOS in urine sample was determined by using the following equation:

$$\text{LOD} = k\text{SDa/b}$$

where  $k=3$ ,  $SDa$  is the standard deviation of the intercept, and  $b$  is the slope. On the basis of 5 replicate measurements, the  $LOD=0.12 \text{ ngml}^{-1}$  was obtained. The respective analytical curve is shown in Figure 12.

In order to evaluate the analytical applicability of the proposed method in the absence and presence of HCTZ in human urine sample, the accuracy and precision were examined. The urine sample was analyzed after spiking by five different concentrations of LOS. The results obtained are summarized in Table 4. As seen in this table, good recoveries were obtained from the procedure, and the presence of HCTZ has no considerable effect on the determination of LOS. In addition, the performance of the designed method in comparison with other techniques is presented in Table 5.

**(Figure 12)**

**(Table 4)**

**(Table 5)**

#### **4. Conclusion**

According to the results, the combination of magnetic solid phase extraction (MSPE), and fluorimetry techniques can be considered as an efficient and sensitive approach to determination of losartan (LOS) in the presence of hydrochlorothiazide (HCTZ) in human urine sample, in part due to rapidity, sensitivity, low cost, and simplicity of the procedures. The influences of common interfering species in human urine sample such as uric acid, oxalate, phosphate, L-leucine, and glucose were investigated. It is found that these species do not significantly interfere with the proposed method. In addition, the presence of HCTZ has no considerable effect on the determination of LOS *via* fluorimetry technique, in part due to no exhibition of fluorescence emission.

The limit of detection (LOD) for LOS by this technique was obtained  $0.12 \text{ ngml}^{-1}$  after optimization of MSPE process.

### **Acknowledgement**

We express our gratitude to Research Center for Pharmaceutical Nanotechnology, Tabriz University of Medical Sciences for supporting this project.

## References

- [1] F. Persson, J. B. Lewis, E. Lewis, P. Rossing, N. K. Hollenberg and H. H. *Clin. J. Am. Soc. Nephro.*, 2011, **6**, 1025-1031.
- [2] D. H. G. Smith, R. Dubiel and M. Jones, *J. Cardiovasc. Drug.*, 2005, **5**, 41-50.
- [3] R. L. Byyny, *J. Hypertens.*, 1995, **13**, S29–S33.
- [4] P. C. Wong, W. A. Price-Jr, A. T. Chiu, J. V. Duncia, D. J. Carini, R. R. Wexler and A. L. Johnson, *J. Pharmacol.*, 1990, **255**, 211–217.
- [5] C. S. Sweet, D. C. Bradstreet, R. S. Berman, N. Jallard, A. Saenz and D. J. Weidler, *J. Hypertens.*, 1994, **7**, 1035–1040.
- [6] P. Sarafidis, P. Georgianos and G. L. Bakris, *Nat. Rev. Nephrol.*, 2013, **9**, 51-58.
- [7] A. Chobanian, *New. Engl. J. Med.*, 2009, **361**, 878-887.
- [8] D. L. Hertzog, J. Finnegan, M. Cafferty, X. Fang, R. J. Tyrrell and R. Ree, *J. Pharmaceut. Biomed. Anal.*, 2002, **30**, 747-760.
- [9] M. Smajic, Z. Vujic and N. Mulavdic, J. Brboric, *Chromatographia*, 2013, **76**, 419–425.
- [10] R. Bonfilio, C. R. T. Tarley, G. R. Pereira, H. R. N. Salgado and M. B. Araujo, *Talanta*, 2009, **80**, 236-241.
- [11] A. B. Thomas, U. B. Chavan, R. K. Nanda, L. P. Kothapalli, S. N. Jagdale, S. B. Dighe and A. D. Deshpande, *Acta Chromatographica.*, 2010, **22**, 219–226.
- [12] R. N. Rao, S. S. Raju, R. M. Vali and G. G. Sankar, *J. Chromatogr B.*, 2012, **902**, 47–54.
- [13] M. Polinko, K. Riffel, H. Song and M. W. Lo, *J. Pharmaceut. Biomed. Anal.*, 2003, **33**, 73-84.

- [14] A. Kumari, H. Prabhakar and R. Giridhar, *J. Pharmaceut. Biomed. Anal.*, 2002, **27**, 861–866.
- [15] S. S. El-Hay, M. Y. El-Mammlı and A. A. Shalaby, *Arab. J. Chem.*, (DOI:10.1016/j.arabjc.2011.06.021).
- [16] I. A. Darwish, *Anal. Chimi. Acta.*, 2005, **549**, 212–220.
- [17] S. B. Etcheverry, E. G. Ferrer, L. Naso, D. A. Barrio, L. Lezama, T. Rojoc and P. M. Williams, *Bioorg. Med. Chem.*, 2007, **15**, 6418–6424.
- [18] M. R. Balesteros, A. F. Faria and M. A. Oliveira, *J. Braz. Chem. Soc.*, 2007, **18**, 554–558.
- [19] Z. Zhang, L. Wang, X. Liu, D. Zhang, L. Zhang and Q. Li, *RSC Adv.*, 2015, **5**, 86445–86452.
- [20] R. Lindberg, G. Fedorova, K. M. Blum, J. P. Prociak, A. Gillman, J. Jarhult, P. Appelblad and H. Soderstrom, *Talanta*, 2015, **141**, 164–169.
- [21] A. A. Asgharinezhad, N. Mollazadeh, H. Ebrahimzadeh, F. Mirbabaei and N. Shekari, *J. Chromatogr A.*, 2014, **1338**, 1–8.
- [22] M. E. Mahmoud, S. B. Ahmed, M. M. Osman and T. M. Abdel-Fattah, *J. Fuel.*, 2015, **139**, 614–621.
- [23] S. Hahn, J. Traeger and H. J. Holdt, *J. Sep. Sci. Technol.*, 2015, **50**, 191–206.
- [24] K. Boddi, A. Taktsy, S. Szabo, L. Mark, L. Mrko, I. Wittmann, R. Ohmacht, G. Montsko, R. M. Vallant, T. Ringer, R. Bakry, C. W. Huck, G. K. Bonn and Z. Szabo, *J. Sep. Sci.*, 2009, **32**, 295–308.
- [25] M. Jaymand, M. Hatamzadeh and Y. Omidı, *Prog. Polym. Sci.*, 2015, **47**, 26–69.
- [26] M. Jaymand, *Prog. Polym. Sci.*, 2013, **38**, 1287–1306.
- [27] Z. Huang and H. K. Lee, *J. Chromatogr A.*, 2015, **1414**, 41–50.

- [28] K. T. Johansen, S. G. Wubshet and N. T. Nyberg, *Anal. Chem.*, 2013, **85**, 3183–3189.
- [29] D. Xiao, C. Zhang, D. Yuan, J. He, J. Wu, K. Zhang, R. Lin and H. He, *RSC Adv.*, 2014, **4**, 64843–64854.
- [30] M. Hatamzadeh, M. Johari-Ahar and M. Jaymand, *Int. J. Nanosci. Nanotechnol.*, 2012, **8**, 51–60.
- [31] C. Huang and B. Hu, *Spectrochim. Acta B.*, 2008, **63**, 437–444.
- [32] A. Dabrowski, *Adv. Colloid. Interfac. Sci.*, 2001, **93**, 135–224.
- [33] I. Langmuir, *J. Am. Chem. Soc.*, 1918, **40**, 1361–1403.
- [34] G. Mckay, H. S. Blair and J. R. Gardener, *J. Appl. Polym. Sci.*, 1982, **27**, 3043–3057.
- [35] H. Bagheri, M. Ahmadi, T. Madrakian and A. Afkhami, *Sens. Actuat B.*, 2015, **221**, 681–687.
- [36] S. Vellaichamy and K. Palanivelu, *J. Hazard. Mater.*, 2011, **185**, 1131–1139.
- [37] H. Bagheri, A. Shirzadmehr and M. Rezaei, *J. Molecul. Liquid.*, 2015, **212**, 96–102.
- [38] L. Abdel-Fattah, L. Abdel-Aziz and M. Gaied, *Spectrochim. Acta A.*, 2015, **136**, 178–184.
- [39] M. C. G. Santos, C. R. T. Tarley, L. H. Dall’Antonia and E. R. Sartori, *Sensor. Actuator B.*, 2013, **188**, 263–270.
- [40] M. Selvadurai and S. N. Meyyanathan, *Pharma. Method.*, 2011, **2**, 95–98.
- [41] M. R. Brunetto, Y. Contreras, S. Clavijo, D. Torres, Y. Delgado, F. Ovalles, C. Ayala, M. Gallignani, J. M. Estela and V. C. Martin, *J. Pharma. Biomed. Anal.*, 2009, **50**, 194–199.

- [42] E. Cagigal, L. Gonzalez, R. M. Alonso and R. M. Jimenez, *Talanta*, 2001, **54**, 1121–1133.
- [43] C. I. Furtek and M. W. Lo, *J. Chromatogr.*, 1992, **573**, 295-301.

**Schemes, Figures, and Tables Captions:**

**Scheme 1.** The chemical structures of LOS and HCTZ.

**Figure 1.** X-ray diffraction pattern of the  $\text{Fe}_3\text{O}_4@\text{SiO}_2\text{-Imz}$  nanoparticles.

**Figure 2.** SEM image of the  $\text{Fe}_3\text{O}_4@\text{SiO}_2\text{-Imz}$  nanoparticles.

**Figure 3.** Magnetization curve of the  $\text{Fe}_3\text{O}_4@\text{SiO}_2\text{-Imz}$  nanoparticles.

**Figure 4.** The effect of the solution pH on the loading efficiency of LOS and HCTZ [pH/Loading efficiency (%)/Relative standard deviation (RSD (%)) for LOS: 3/65/2.76; 4/67/3.28; 5/71/3.66; 6/85/2.82; 7/93/3.01; 8/99/2.12; 9/94/2.87; 10/90/2.77, and for HCTZ: 3/40/4.25; 4/42/4.52; 5/43/4.65; 6/44/4.77; 7/45/5.11; 8/44/5.00; 9/43/5.58; 10/45/5.77].

**Figure 5.** The effect of adsorbent amount on the loading efficiency of LOS [Adsorbent (mg)/ Loading efficiency (%)/RSD (%): 0.25/30/6.33; 0.50/50/3.40; 0.75/85/2.47; 1/99/1.81; 1.25/99/2.22; 1.5/99/1.67].

**Figure 6.** The effect of the contact time on the loading efficiency of LOS [Time (min)/Loading efficiency (%)/RSD (%): 5/71.9/1.94; 6/77.2/1.68; 7/87.8/1.93; 8/93/1.29; 9/98.3/1.52; 10/99/1.62; 11/98.6/1.31; 12/99/1.21; 15/98.5/1.62].

**Figure 7.** Langmuir adsorption isotherm of LOS onto  $\text{Fe}_3\text{O}_4@\text{SiO}_2\text{-Imz}$  nanoparticles.

**Table 1.** Adsorption isotherms parameters of LOS onto  $\text{Fe}_3\text{O}_4@\text{SiO}_2\text{-Imz}$  nanoparticles.

**Table 2.** Desorption efficiency of LOS from  $\text{Fe}_3\text{O}_4@\text{SiO}_2\text{-Imz}$  nanoparticles with different organic solvents.

**Figure 8.** The effect of desorption solvent volume (methanol/NaOH (20%w/v)) on the recovery efficiency of the LOS [Eluent (ml)/Desorption (%)/RSD (%): 0.50/40/3.5; 0.75/65/2.61; 0.80/75/1.73; 0.90/90/2.11; 1/98/1.42; 1.25/96/1.56; 1.5/99/1.31; 2/98/1.63].

**Figure 9.** The optimization of desorption time [Time (min)/Desorption (%)/RSD (%): 5/74.2/1.75; 8/82.1/1.70; 10/90.6/1.43; 13/95.9/1.25; 14/97.5/1.33; 15/98/1.12; 16/98.1/1.01; 17/98.2/1.22; 18/97.9/1.43; 20/98/1.22].

**Figure 10.** The effect of the sample volume on desorption of LOS from Fe<sub>3</sub>O<sub>4</sub>@SiO<sub>2</sub>-Imz nanoparticles [Sample volume (ml)/Loading (%)/RSD (%): 10/99/1.41; 50/99/1.21; 100/98/1.30; 150/97/0.73; 200/96/0.80; 220/96/0.54; 250/95/0.60; 260/94/0.61; 300/90/0.26; 350/75/0.54].

**Figure 11.** The excitation (a), and emission (b) fluorescence ( $\lambda_{exc}=250$  nm,  $\lambda_{emi}=325$  nm) spectra of the LOS.

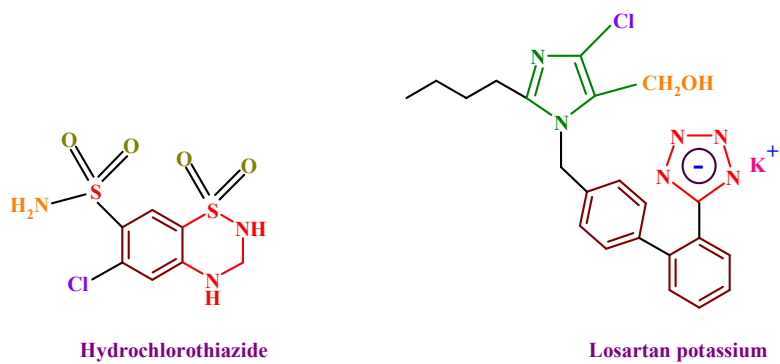
**Table 3.** The effects of common interfering species on the determination of LOS (0.1 mg l<sup>-1</sup>).

**Figure 12.** The analytical curve for determination of LOS.

**Table 4.** Recovery, intraday-RSD, and interday-RSD for LOS in urine sample at different concentrations.

**Table 5.** Performance comparison of the designed method with other techniques.

## Schemes, Figures, and Tables:



**Scheme 1.** The chemical structures of LOS and HCTZ.

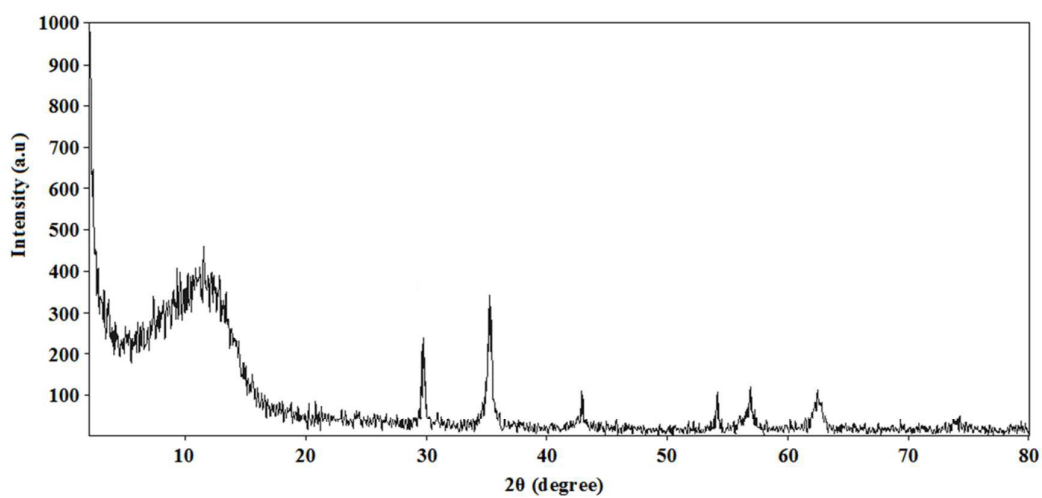


**Figure 1.** X-ray diffraction pattern of the Fe<sub>3</sub>O<sub>4</sub>@SiO<sub>2</sub>-Imz nanoparticles.

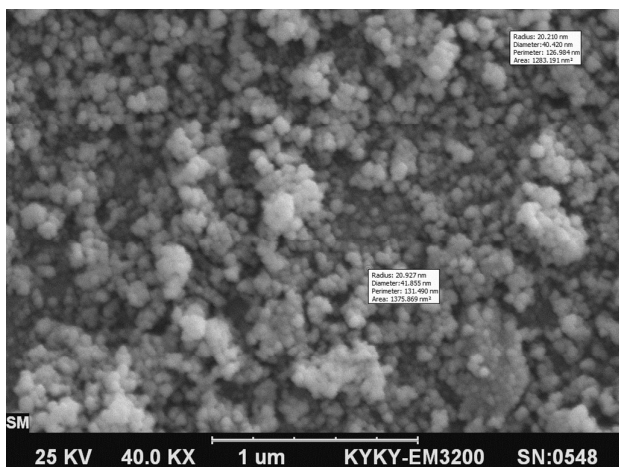


**Figure 2.** SEM image of the Fe<sub>3</sub>O<sub>4</sub>@SiO<sub>2</sub>-Imz nanoparticles.

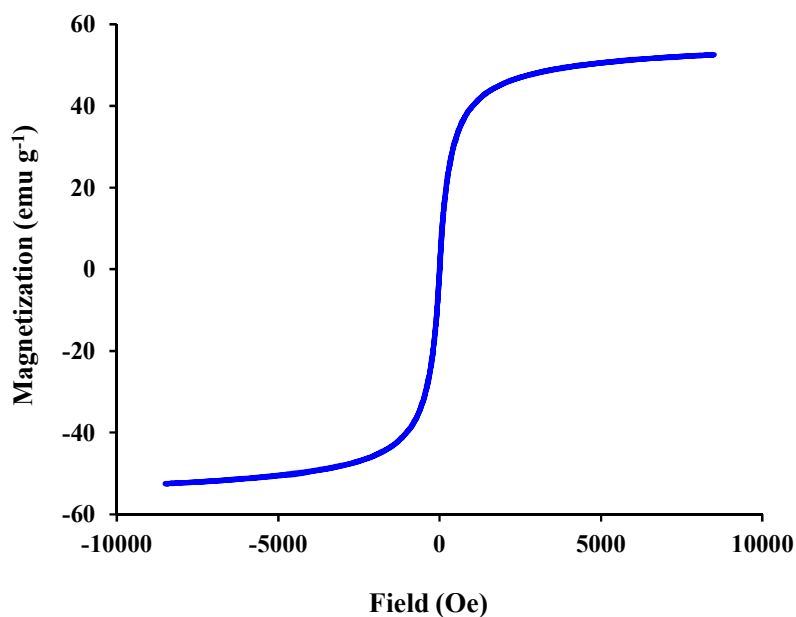


**Figure 3.** Magnetization curve of the Fe<sub>3</sub>O<sub>4</sub>@SiO<sub>2</sub>-Imz nanoparticles.

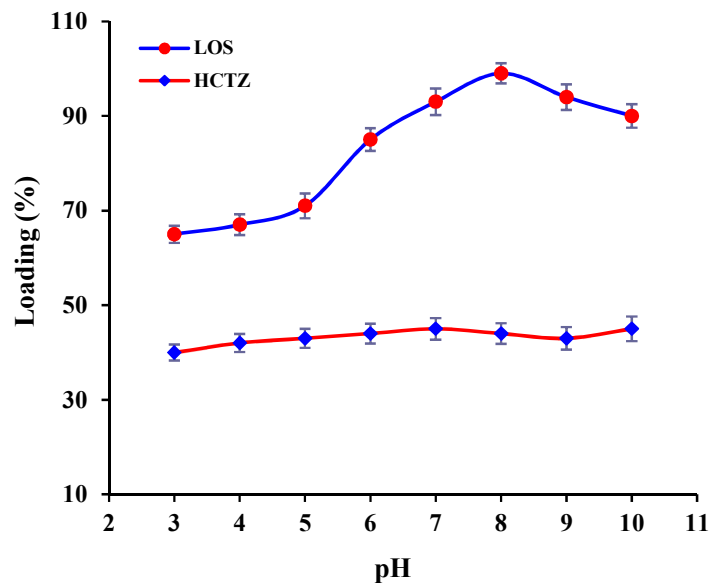


**Figure 4.** The effect of the solution pH on the loading efficiency of LOS and HCTZ [pH/Loading efficiency (%) /Relative standard deviation (RSD (%)) for LOS: 3/65/2.76; 4/67/3.28; 5/71/3.66; 6/85/2.82; 7/93/3.01; 8/99/2.12; 9/94/2.87; 10/90/2.77, and for HCTZ: 3/40/4.25; 4/42/4.52; 5/43/4.65; 6/44/4.77; 7/45/5.11; 8/44/5.00; 9/43/5.58; 10/45/5.77].

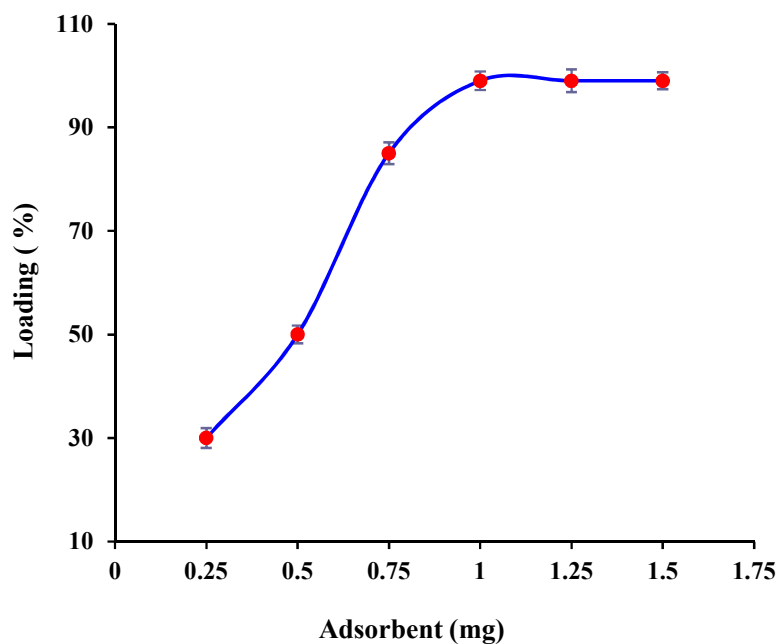


**Figure 5.** The effect of adsorbent amount on the loading efficiency of LOS  
[Adsorbent (mg)/ Loading efficiency (%)/RSD (%): 0.25/30/6.33;  
0.50/50/3.40; 0.75/85/2.47; 1/99/1.81; 1.25/99/2.22; 1.5/99/1.67].

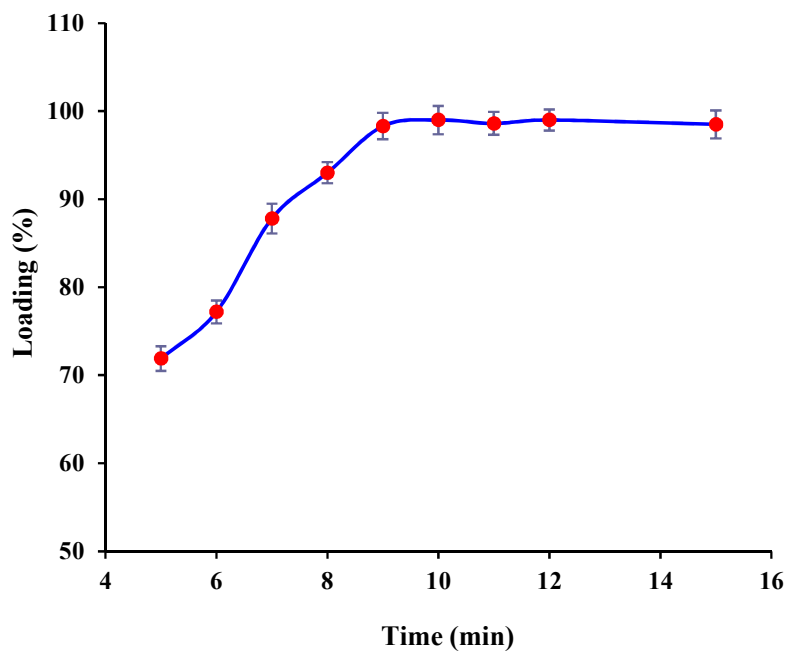


**Figure 6.** The effect of the contact time on the loading efficiency of LOS [Time (min)/Loading efficiency (%) /RSD (%): 5/71.9/1.94; 6/77.2/1.68; 7/87.8/1.93; 8/93/1.29; 9/98.3/1.52; 10/99/1.62; 11/98.6/1.31; 12/99/1.21; 15/98.5/1.62].

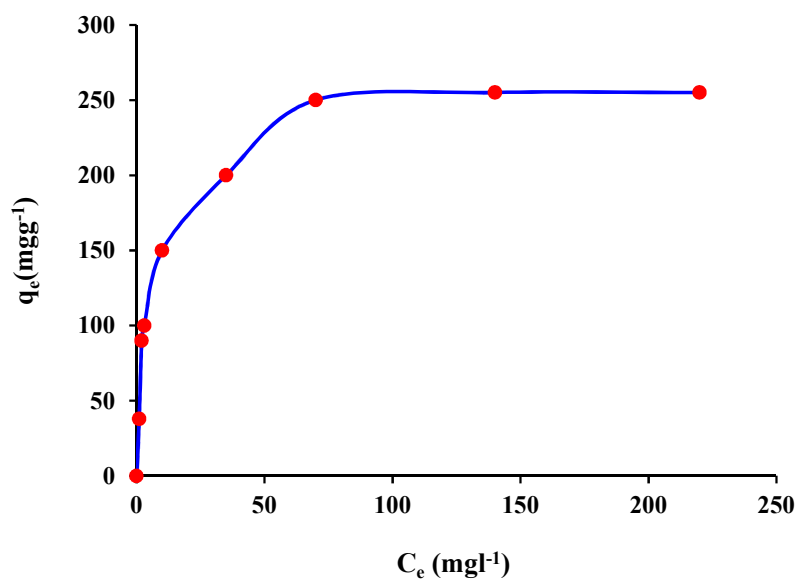


**Figure 7.** Langmuir adsorption isotherm of LOS onto  $\text{Fe}_3\text{O}_4@\text{SiO}_2\text{-Imz}$  nanoparticles.

**Table 1.** Adsorption isotherms parameters of LOS onto  $\text{Fe}_3\text{O}_4@\text{SiO}_2\text{-Imz}$  nanoparticles.

sample	$q_{\text{max}}$ (mg g <sup>-1</sup> )	$b$ ( $K_L q_{\text{max}}^{-1}$ )	$K_L$ (l mg <sup>-1</sup> )	$r$
Losartan	260	0.370	73.90	0.992

**Table 2.** Desorption efficiency of LOS from Fe<sub>3</sub>O<sub>4</sub>@SiO<sub>2</sub>-Imz nanoparticles with different organic solvents.

solvent	Desorption efficiency (%)
Acetonitrile	92
Methanol	95
Ethanol	85
Dioxane	60
<i>n</i> -Hexane	50
Methanol/NaOH (20% w/v)	98

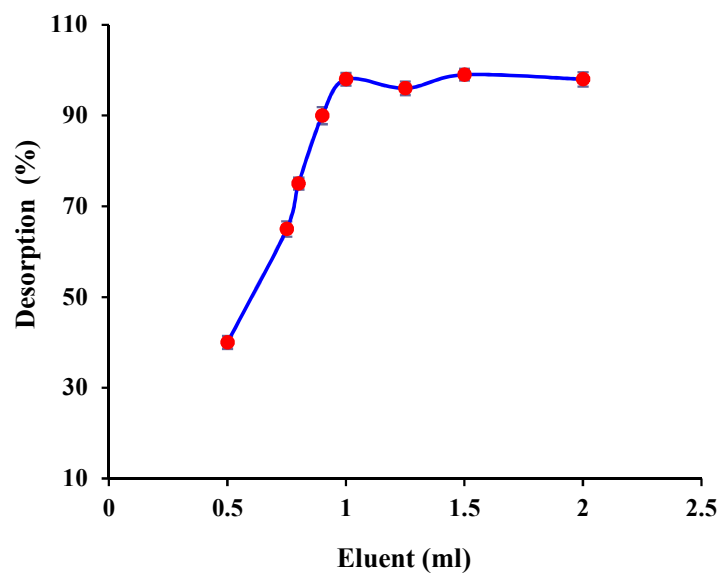


**Figure 8.** The effect of desorption solvent volume (methanol/NaOH (20%w/v)) on the recovery efficiency of the LOS [Eluent (ml)/Desorption (%)/RSD (%): 0.50/40/3.5; 0.75/65/2.61; 0.80/75/1.73; 0.90/90/2.11; 1/98/1.42; 1.25/96/1.56; 1.5/99/1.31; 2/98/1.63].

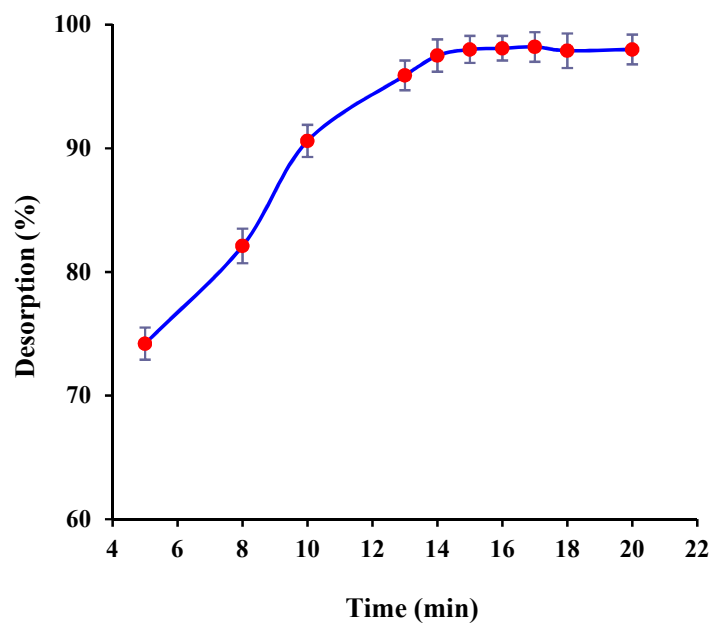


**Figure 9.** The optimization of desorption time [Time (min)/Desorption (%)/RSD (%):

5/74.2/1.75; 8/82.1/1.70; 10/90.6/1.43; 13/95.9/1.25; 14/97.5/1.33;

15/98.1/1.12; 16/98.1/1.01; 17/98.2/1.22; 18/97.9/1.43; 20/98/1.22].

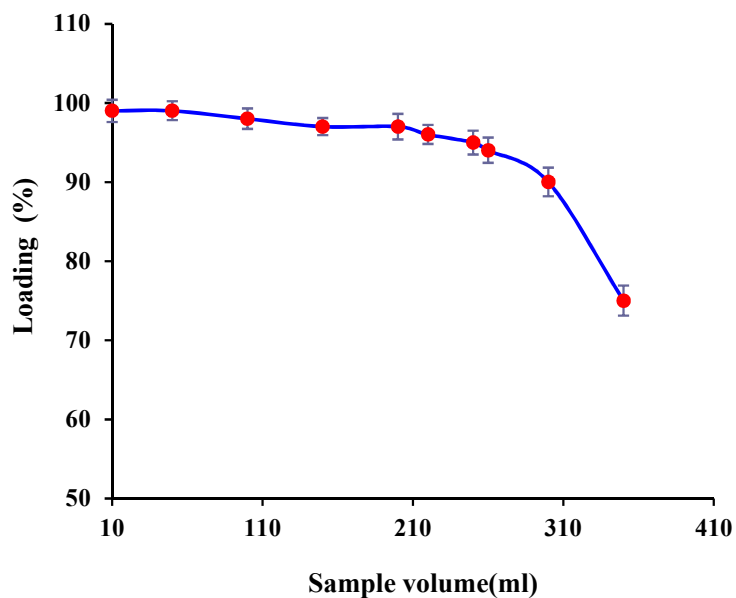


**Figure 10.** The effect of the sample volume on desorption of LOS from  $\text{Fe}_3\text{O}_4@\text{SiO}_2\text{-Imz}$  nanoparticles [Sample volume (ml)/Loading (%)/RSD (%): 10/99/1.41; 50/99/1.21; 100/98/1.30; 150/97/0.73; 200/96/0.80; 220/96/0.54; 250/95/0.60; 260/94/0.61; 300/90/0.26; 350/75/0.54].

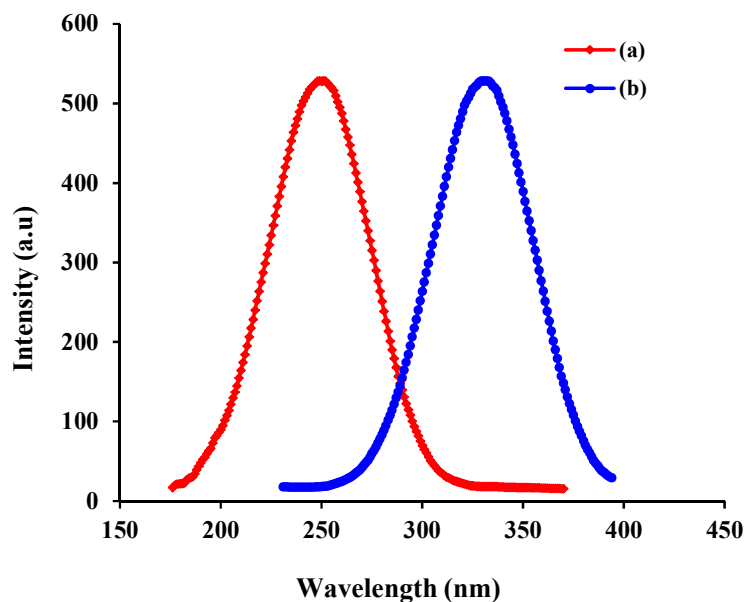


**Figure 11.** The excitation (a), and emission (b) fluorescence ( $\lambda_{\text{exc}}=250$  nm,  $\lambda_{\text{emi}}=325$  nm) spectra of the LOS.

**Table 3.** The effects of common interfering species on the determination of LOS ( $0.1 \text{ mg l}^{-1}$ ).

Interfering species	Concentration ( $\text{mg l}^{-1}$ )	$\Delta F$ variation (%) <sup>a</sup>
Uric acid	0.01	-4.2
Oxalate	0.005	-3.2
Phosphate	0.003	-3.5
L-Leucine	120.00	2.5
Glucose	100.00	3.0

<sup>a</sup> Fluorescence intensity ( $\Delta F$ ).

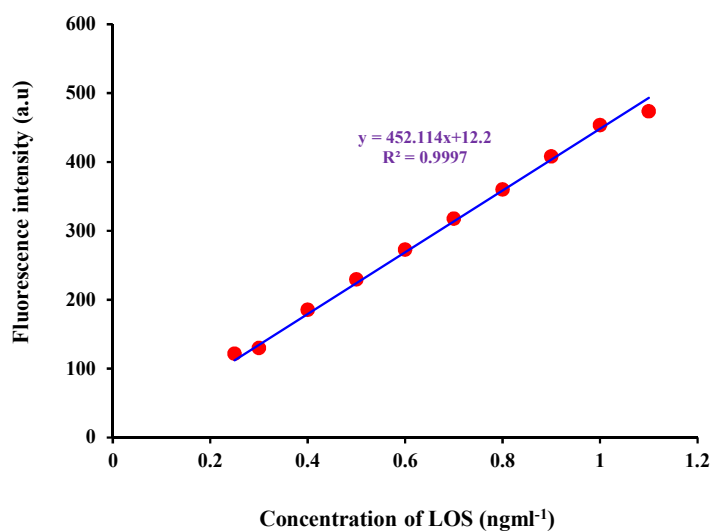


**Figure 12.** The analytical curve for determination of LOS.

**Table 4.** Recovery, intraday-RSD, and interday-RSD for LOS in urine sample at different concentrations.

Spiked value of LOS (ngml <sup>-1</sup> )	Spiked value of HCTZ (ngml <sup>-1</sup> )	Founded value (ngml <sup>-1</sup> )	Intraday-RSD (%) (n=5)	Interday-RSD (%) (n=5)	Recovery of LOS (%)
1	1	1.10	6.5	6.8	110
5	-	4.80	2.5	4.5	96
10	5	10.10	2.3	4.1	101
25	-	24.80	0.9	1.6	99.2
50	30	49.70	0.5	1.2	99.4

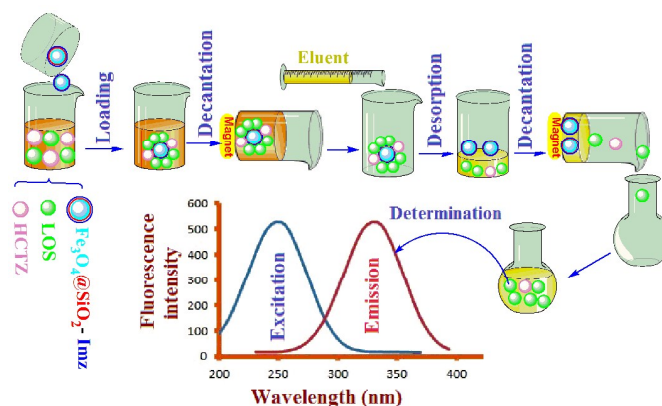
**Table 5.** Performance comparison of the designed method with other techniques.

Determination method	LOD	Reference
Suggested method (SPE-fluorimetry)	0.12 ngml <sup>-1</sup>	This work
Potentiometry	77 ngml <sup>-1</sup>	37
Spectrophotometry	0.5–28 µgml <sup>-1</sup>	38
Voltammetry	4.1 µgml <sup>-1</sup>	39
Liquid chromatography–mass spectrometric	1.0 ngml <sup>-1</sup>	12
High-performance thin-layer chromatography	1.190 µgml <sup>-1</sup>	40
Reversed phase HPLC	0.114 mgml <sup>-1</sup>	10
Liquid chromatography-fluorescence spectroscopy	2.0 ngml <sup>-1</sup>	41
Liquid chromatography-tandem mass spectrometry	1 ngml <sup>-1</sup>	13
Fluorescence spectroscopy	0.5 µgml <sup>-1</sup>	42
HPLC	20 ngml <sup>-1</sup>	43

## Determination of losartan potassium in the presence of hydrochlorothiazide *via* combination of magnetic solid phase extraction, and fluorimetry techniques in urine sample

Amir Farnoudian-Habibi<sup>1</sup>, Sahar Kangari<sup>2</sup>, Bakhshali Massoumi<sup>3</sup>, and Mehdi Jaymand<sup>\*,1</sup>

1. Research Center for Pharmaceutical Nanotechnology, Tabriz University of Medical Sciences, P.O. Box: 51656-65811, Tabriz, Islamic Republic of Iran.
2. Department of Chemistry, Science and Research Branch, Islamic Azad University, P.O. Box: 14515-775, Tehran, Islamic Republic of Iran.
3. Department of Chemistry, Payame Noor University, P.O. BOX: 19395-3697, Tehran, Islamic Republic of Iran.



A sensitive and highly efficient method for determination of losartan potassium (LOS) in the presence of hydrochlorothiazide (HCTZ) *via* combination of magnetic solid phase extraction (MSPE), and fluorimetry techniques is suggested.

\* Correspondence to: Mehdi Jaymand, Research Center for Pharmaceutical Nanotechnology, Tabriz University of Medical Sciences, Tabriz, Islamic Republic of Iran.

Tel: +98-41-33367914; Fax: +98-41-33367929

Postal address: Tabriz-5165665811-Iran

E-mail addresses: [m\\_jaymand@yahoo.com](mailto:m_jaymand@yahoo.com); [m.jaymand@gmail.com](mailto:m.jaymand@gmail.com); [jaymandm@tbzmed.ac.ir](mailto:jaymandm@tbzmed.ac.ir)